Cross-section high resolution transmission electron microscopy and nanoprobe investigations of gallium nitride nanowires

Benjamin W. Jacobs

Michigan State University,
East Lansing, Michigan, 48824, USA
and
Sandia National Laboratories,
Livermore, CA 94551-0969, USA
E-mail: bjacobs@sandia.gov

Kaylee McElroy, Raed A. Al-Duhaileb, Martin A. Crimp and Virginia M. Ayres*

Michigan State University,
East Lansing, Michigan, 48824, USA
E-mail: mcelro11@msu.edu
E-mail: alduhail@msu.edu
E-mail: crimp@egr.msu.edu
E-mail: ayresv@msu.edu
*Corresponding author

Richard E. Stallcup

Zyvex Instruments,
Richardson, TX, 75081, USA
E-mail: rstallcup@zyvex.com

Adam B. Hartman

Zyvex Instruments,
Richardson, TX, 75081, USA
and
Siemens Energy & Automation,
Arlington, TX, USA
E-mail: adam.hartman@seimens.com

Mary Anne Tupta

Keithley Instruments, Inc.,
Cleveland, OH, 44139, USA
E-mail: mtupta@keithley.com

Abstract: Gallium nitride nanowires and rods were grown by a vapour-solid growth mechanism over an 850–1,000°C furnace growth temperature range. Investigations by parallel (cross-section) high resolution transmission electron microscopy revealed correlated internal structures. The effects of the internal structures on electronic properties were investigated by micro- and nano-probe experiments. A space-charge limited interpretation of the observed non-linear I–V behaviour is examined.

Keywords: gallium nitride nanowire; multiphase nanowire; internal structure; transmission electron microscopy; high resolution transmission electron microscopy; HRTEM; focussed ion beam; FIB; cross-section; nanoelectronics; nanoprobes.

Reference to this paper should be made as follows: Jacobs, B.W., McElroy, K., Al-Duhaileb, R.A., Crimp, M.A., Ayres, V.M., Stallcup, R.E., Hartman, A.B. and Tupta, M. (2010) 'Cross-section high resolution transmission electron microscopy and nanoprobe investigations of gallium nitride nanowires', *Int. J. Nanomanufacturing*, Vol. 6, Nos. 1/2/3/4, pp.264–278.

Biographical notes: Benjamin W. Jacobs received his BS and PhD in Electrical Engineering and a concurrent BA in German Language and Culture Studies from Michigan State University, East Lansing, Michigan, USA. He was awarded a NASA Graduate Student Researchers Program Fellowship 2004–2007 for research in structures and electronic properties of multiphase GaN nanowires and carbon nanomaterials. He is currently a Post-doctoral Appointee at Sandia National Laboratories in Livermore, CA, USA, working with nanoporous materials for energy storage and generation.

Kaylee McElroy is currently a Master's degree candidate in Electrical Engineering at Michigan State University, USA. Her research interests include crystal nucleation and growth of III-V semiconductor nanowires and tribological properties of carbon nanomaterials. She received her BS in Physics with Senior Honours Thesis from Brigham Young University, Provo, UT, USA and a National Science Foundation NNIN REU award for investigations of GaN nanowires at the Cornell Nanoscale Science and Technology Center, Ithaca, NY, USA.

Raed A. Alduhaileb received his BS in Electrical Engineering from Kind Fahd University of Petroleum and Minerals (Dhahran, Saudi Arabia) in 2004. He is currently a Master's degree candidate in Electrical Engineering at Michigan State University, USA, where he is awarded a full graduate scholarship from the national oil company of Saudi Arabia (Saudi Aramco). His research interests include tribological and electronic properties of carbon nanomaterials in extreme environments.

Martin A. Crimp is a Professor in the Department of Chemical Engineering and Materials Science at Michigan State University, East Lansing, MI, USA, with extensive interests in electron microscopy investigation, both scanning and transmission, of advanced materials. His research interests include dislocation-based deformation mechanisms in structural metals using both diffraction and phase contrast. He has extensively used SEM electron channelling techniques for crystallographically-based imaging of dislocations and twins in bulk materials. Other materials systems of interest include giant magnetoresistance (GMR) multilayers and spinvalves, rare-earth silicide nanostructures, multiphase GaN nanowires and carbon nanomaterials in extreme environments.

Virginia M. Ayres is an Associate Professor in the Department of Electrical & Computer Engineering, and heads the Electronic and Biological Nanostructures Laboratory (http://www.egr.msu.edu/ebnl) at Michigan State University, East Lansing, MI, USA. Her research interests include electronic properties of reduced dimensionality semiconductor nanowires and carbon nanomaterials in normal and in extreme environments. She received her PhD and MS in Physics from Purdue University, West Lafayette, IN, USA and concurrent BAs in Physics and in Biophysics from the Johns Hopkins University, Baltimore, MD, USA.

Richard E. Stallcup II, is the Lead Applications Development Staff Scientist for NanoWorks™ tools at Zyvex Instruments, Richardson, TX, USA. His research interests include in situ nanomanipulation for nanomaterials engineering with direct TEM or SEM visualisation and novel nanoprobe technologies for low noise electronic investigations of nanostructures and individual IC transistors. He received his PhD in Physics from the University of North Texas, Denton, TX. USA.

Adam B. Hartman is currently a Product Design Engineer with Siemens Energy and Automation, Arlington TX, USA and formerly a Mechanical Engineer for Applications Development with Zyvex Instruments, Richardson, TX, USA. His research interests include nano robotics, MEMS design and mechanical and electrical testing of nanostructures and individual IC transistors. He received a BS from Rose-Hulman Institute of Technology, Terre Haute, IN, USA and was a Graduate Researcher in the MEMS group in the Department of Mechanical Engineering at University of Colorado, Boulder, CO, USA.

Mary Anne Tupta is a Senior Applications Engineer at Keithley Instruments, Inc. in Cleveland, Ohio. She received the MS in Physics and a BS in Physics/Electronic Engineering from John Carroll University, Cleveland, OH, USA. Her research interests include development of low-noise electronic measurement techniques for investigations of nanostructures and individual IC transistors.

1 Introduction

Semiconducting nanowires represent a new class of device building blocks with properties enhanced by their small size and large aspect ratios. Gallium nitride (GaN) nanowires in particular have received much attention due to their unique material properties. GaN nanowire-based blue/UV lasers are an especially desirable application under investigation by several groups (Hersee et al., 2006; Gradecak et al., 2005; Johnson et al., 2002; Huang et al., 2001). To date, optical pumping of GaN nanowire lasers has been successfully demonstrated; however electronic pumping for a compact, all solid-state device has not yet been realised. Electronic pumping requires well-defined energy states in a highly crystalline material as an essential characteristic for efficient lasing action. GaN nanowires are also being explored for electronic device applications, where highly crystalline nanowires are needed to optimise device performance.

Nanowires are known for their high crystallinity. However, very recent results (Hersee et al., 2006; Gradecak et al., 2005; Johnson et al., 2002; Huang et al., 2001;

Bierman et al., 2008; Mikkelsen et al., 2004; Tham et al., 2006) indicate that nanowires may possess an internal structure, which is not readily apparent even with investigation by plan-view (perpendicular) high resolution transmission electron microscopy (HRTEM). In the present investigations, GaN nanowires and rods were analysed with plan-view (perpendicular) and cross-section (parallel) HRTEM. Details of the cross-section process are described in detail in Jacobs et al. (2008a, 2008b). The cross-section studies revealed details of the internal structures of GaN nanowires and rods that would have been difficult to reconstruct from plan-view HRTEM alone.

The effects of the internal structures on electronic properties were investigated by two-point microprobe and two- and four-point nanoprobe experiments. For these experiments, GaN nanowire nanocircuits were fabricated using electron beam lithography, as described in Jacobs et al. (2007a).

2 Results and discussion

2.1 Internal structure investigations

The GaN nanowires and rods used in this study were synthesised by a catalyst-free direct reaction of gallium vapour and ammonia (He et al., 2001). Nanowires and rods with two orientations were obtained using this growth method, approximately dependent on the furnace growth temperature. At furnace growth temperatures 850°C and 950°C, unique multiphase zinc-blende/wurtzite GaN nanowires with triangular cross-sections, ranging between 60–150 nm in width with growth orientations along the <011> direction for zinc-blende and the <2-1-10> direction for wurtzite were commonly obtained (Jacobs et al., 2007b, 2008a). The multiphase nanowires had multiple highly crystalline zinc-blende and wurtzite domains that extended along the entire length of the nanowire. Extensive plan-view TEM of over 50 nanowires to date was used to check that the multiphase character extends over the full length of the nanowire. At furnace growth temperatures of 1,000°C, single-phase wurtzite GaN nanowires and rods with hexagonal cross sections, ranging between 200–5000 nm in width, with growth orientation along the [0001] direction were commonly obtained (Jacobs et al., 2008b).

Cross-sections for HRTEM were fabricated using a focused ion beam (FIB, FEI Quanta 200 3D) system. The HRTEM analysis of a cross-section taken from a nanowire grown at 850°C is shown in Figure 1. Three ~30 nm wurtzite domains and one ~40 nm zinc-blende domain are evident. A long (~80 nm) coherent interface between wurtzite region 4 and zinc-blende region 5 is observed in the image and verified by the Fast Fourier Transforms (FFTs) of regions 4 and 5, shown right. Also, the triangular region 2, discussed in detail in Jacobs et al. (2008a), is a small wurtzite region with smaller zinc-blende ‘spacers’ at each apex that enable it to fit smoothly with regions 1, 3 and 4. Three short ~10 nm coherent interfaces (not shown) were observed between the zinc-blende and wurtzite components of region 2.

The HRTEM analysis of a cross-section taken from a nanowire grown at 950°C is shown in Figure 2. Three larger ~30 nm wurtzite domains and one smaller ~20 nm zinc-blende domain are evident. Wurtzite domains 2 and 3 are separated into a, b regions by the development of stacking faults in each, indicated as a dotted line. Region 2a shares

a totally coherent (0001)/(111) interface with zinc-blende region 1, indicated by the horizontal arrows in the FFTs, right. Furthermore, regions 3b and 3c are almost coherent with each other as well as with zinc-blende region 1 between them, as shown by the FFTs, right. Stacking fault regions are observed between regions 3b and 1 and regions 3c and 1. The character of the stacking fault regions is mixed wurtzite/zinc-blende, rather than random disorder.

All cross sections of multiphase GaN nanowires grown at furnace temperatures of 850–950°C examined to date involved one or more coherent interfaces between zinc-blende {111} planes and wurtzite (0001) planes at domain interfaces. Coherent domain interfaces are considered to be important for the structural stability of the multiphase nanowires. Nanowire nucleation and growth is discussed below. It is noted here that a zinc-blende nucleation site for step-ledge growth has not yet been identified. The results shown above suggest the possibility that the formation of the zinc-blende regions may be driven by lowering of internal stresses.

Figure 1 HRTEM of cross-section of GaN nanowire grown at 850°C (see online version for colours)

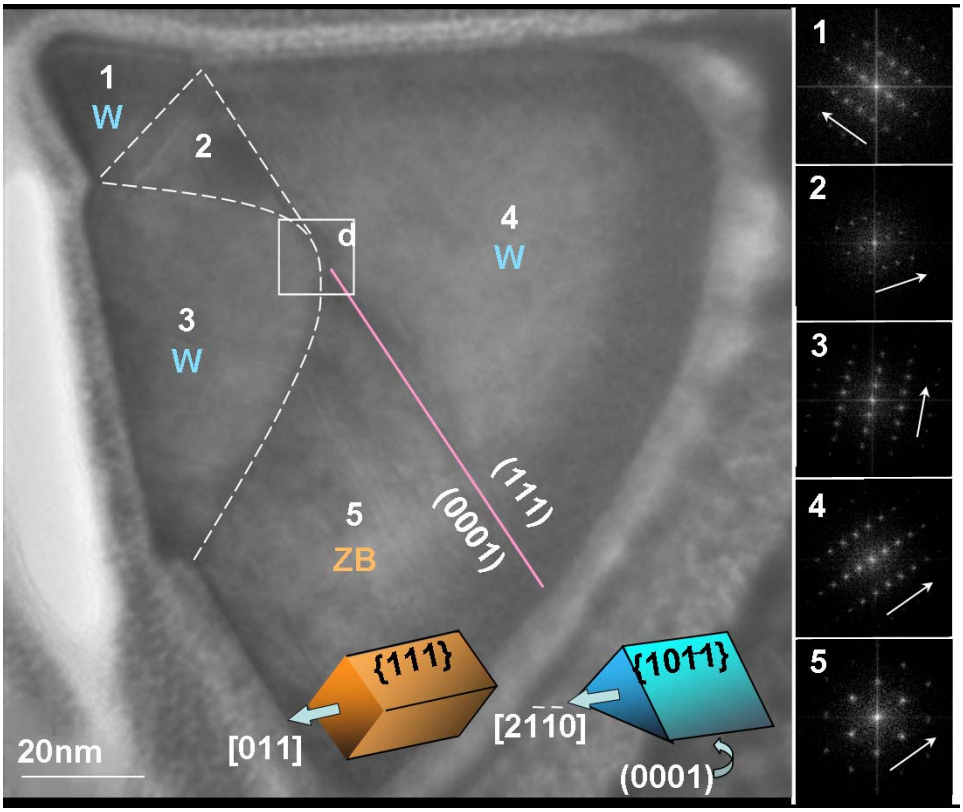

Note: The totally coherent wurtzite/zinc-blende interface is indicated by the straight line.

Source: adapted from Figure 2, Jacobs et al. (2008a)

Figure 2 HRTEM of cross-section of GaN nanowire grown at 950°C (see online version for colours)

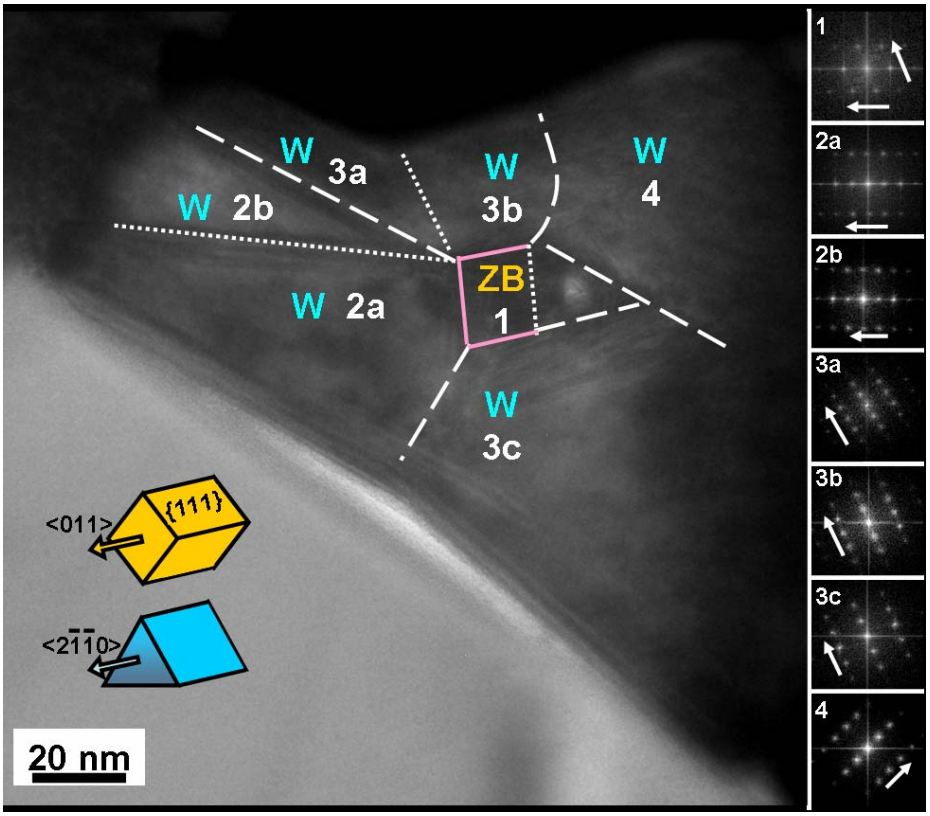

Note: The totally coherent wurtzite/zinc-blende interface between regions 2a and 1 and the almost coherent interfaces between regions 3a-1-3c are indicated by straight lines.

GaN nanowires and rods grown at 1,000°C were single-phase wurtzite GaN with [0001] growth orientation, determined by selected area electron diffraction, as shown in Figures 3(a)–3(c). A detailed HRTEM investigation of a cross-section of a fortunate parallel growth of four rods and two nanowires is presented in Jacobs et al. (2008b). A hexagonal core located at or near the centre was observed in all nanowires and rods. Spiral bend contours resulting from an axial screw dislocation, shown in Figure 3(a), were observed in rods whose cross-sections were sufficiently thin to enable resolution of lattice fringes. The hexagonal core regions shown in Figures 3(d) and 3(e) were partially to totally electron transparent indicating the formation of a hollow core. The interface between the two rods of Figure 3(a) is shown in the inset. It consisted of 5–7 atomic layers of stacking faults along the {10-10} planes. It was also noted that, at the interface, the bend contours appeared to balance each other.

The formation of a hollow core or nanopipe from a screw dislocation with a giant Burgers vector was predicted for thin cylinders by Frank (1951) and Eshelby (1953) and Eshelby and Stroh (1951). Their mathematical conditions are now experimentally

realised in nanowires. There is emerging evidence that nanopipe formation may occur in a variety of different nanowire types (Bierman et al., 2008; Jacobs et al., 2008b). If confirmed as a general trend, axial screw dislocation mechanisms, with the possibility of hollow core formation, will significantly impact nanowire device design, especially nanowire laser design.

Figure 3 HRTEM of cross-section of parallel growth of two GaN rods grown at 1,000°C

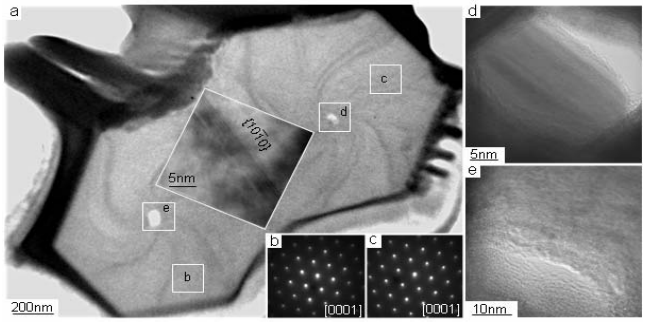

Note: Bend contours are evidence of a screw dislocation. A central hexagonal region in each is partially to totally electron transparent indicating formation of a hollow core.

Source: adapted from Figure 2, Jacobs et al. (2008b)

2.2 Nucleation mechanism investigations

Understanding the vapour-solid nucleation mechanisms is important for controlled growth of nanowires. Growth of the nanowires and rods in these studies was catalyst-free: no metallic catalyst was deliberately introduced for vapour-liquid-solid growth. No evidence for self-catalyzed growth through the development of puddles of liquid Ga has been observed to date. Therefore, it is assumed that the GaN nanowires and rods in these investigations have grown by a vapour-solid mechanism (Kuykendall et al., 2004). During growth, an amorphous film forms first, followed by the development of a growth matrix of microcrystalline GaN platelets (He et al., 2001). Nanowire growth is initiated following formation of the microcrystalline growth matrix. The change in the nanowire growth direction from wurtzite <2-1-10>/zinc-blende <011> directions at 850°C and 950°C to the wurtzite [0001] direction at 1,000°C has been discussed above. Scanning electron microscopy (Hitachi S-4700 II Field Emission SEM) investigation showed that the GaN matrix from which the nanowires grow underwent a parallel evolution at the three furnace growth temperatures. Representative growth matrix SEM images are shown in Figure 4. At 850°C, the matrix consisted of a relatively uniform group of ~1 μm platelets, as shown in Figure 4(a). The matrix that formed at 950°C was similar to the one that formed at 850°C, as shown in Figure 4(b). However, at 1,000°C, three distinct matrix types were observed to form, as shown in Figure 4(c). Type 1 had large 1–20 μm crystallites of GaN. A few large rods with cross sections between 0.5 and 20 μm formed from this type of matrix. No nanowires with diameters less than 100 nm were observed growing from these parts of the matrix. Type 2 matrix had medium sized 0.1–1 μm platelets with observed nanowire growth. The Type 2 matrix in the 1,000°C growth appeared comparable to the matrix for 850°C and 950°C. The Type 3 matrix consisted of

small nanocrystalline platelets around 50–300 nm wide. NW growth was also observed from these nanocrystalline platelets. The overall density of nanowires on the top surface of the 1,000°C matrix was lower than the others, as only rods grew on Type 1 matrix.

Figure 4 SEM investigation of the growth matrix for vapour-solid growth of nanowires shows evolution as a function of furnace growth temperature (a) 850°C (b) 950°C and (c) 1,000°C

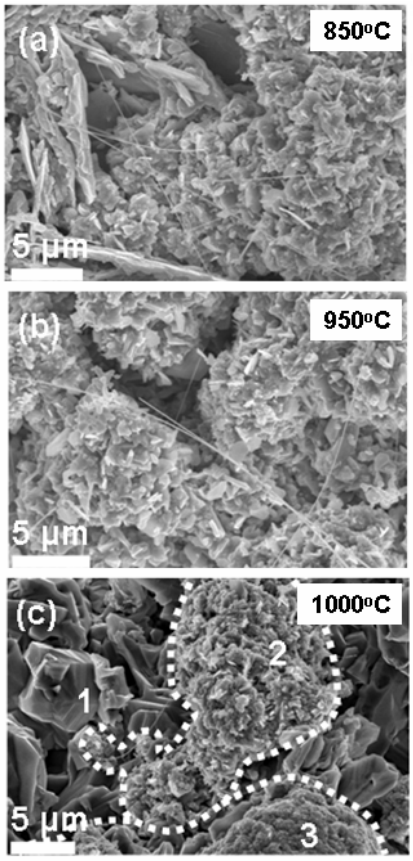

The ~1 μm platelet growth matrix for 850°C and 950°C was investigated by HRTEM. Energy dispersive x-ray spectroscopy (EDS) (not shown) and selected area electron diffraction (shown in the insets) indicated that the growth matrix was stoichiometric wurtzite GaN. The micron-scale platelets had networks of triangular nanoscale ledges in the same orientation and coherent to the main platelet formation, shown in Figure 5. The apex points of the nanoscale ledges were oriented in the <2-1-10> direction (a-direction), as shown in Figures 5(a) and 5(b). This is was the same orientation as the wurtzite phase in the multiphase nanowire growth. The points of the nanoscale ledges would be expected to be potential nucleation sites for vapour-solid growth. If just the apex point contributed to nanowire nucleation, the nanowires would be expected to be thinner than observed. However, NH_3 is known to break down at step edges, forming a source of nitrogen radicals. Surface nitrogen may then be abstracted forming molecular nitrogen, leading to a decomposition process on the surface of the nanoscale ledges. Bombardment of the

nanoscale ledges by energetic gallium atoms may also contribute to the decomposition process. This in turn could lead to a line of dangling bonds on the {2-1-10} planes, which would be expected to be very active sites. Evidence of decomposed nanoscale ledges oriented in the <2-1-10> direction has been reported in detail in Jacobs et al. (2008a).

Growth would be also expected along the {10-10} ledges (m-direction) shown in Figure 5(c) and (d). Competitive {10-10} wurtzite growth was frequently observed near nanowire nucleation sites, resulting in blade-like structures [10]. However, growth along the fastest-growth <2-1-10 > wurtzite and <011> zinc-blende directions appears to eventually dominate nanowire growth.

Figure 5 HRTEM investigations of the nanowire growth matrix at 850°C and 950°C revealed a network of nanoscale ledges that could serve as nucleation sites for nanowire growth

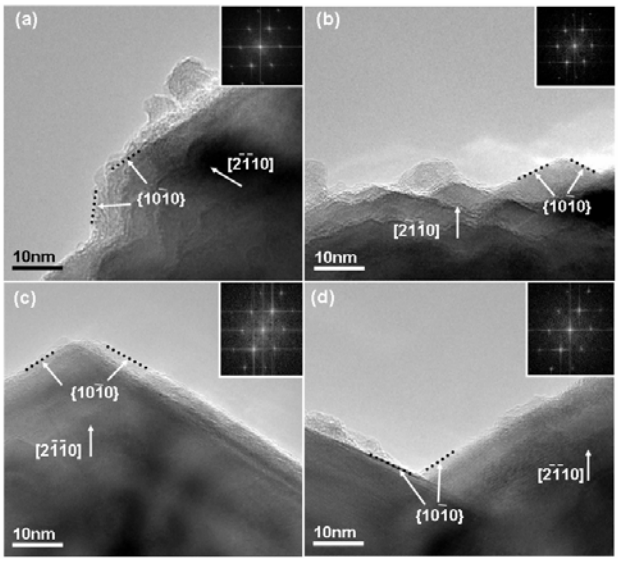

Nucleation at multiple nanoscale ledge sites could explain the multiple wurtzite domains as multiple nanoscale ledges could contribute to a single nanowire. The electron transparency of the nanoscale ledges indicated that they were about 30 nm thick, which is close to the observed wurtzite domain size. The <2-1-10> orientation of the nanoscale ledge sites is consistent with vapour-solid growth of <2-1-10> orientation wurtzite domains. The expected competitive {10-10} growth has been observed (Jacobs et al., 2008a). These observations support the hypothesis that the nanoscale ledges may act as the nucleation sites for vapour-solid growth of multiphase GaN nanowires.

The nucleation sites for the [0001] oriented rods and nanowires grown at 1,000°C are currently under investigation by our group. There is evidence that nucleation from (0001) faces of hexagonal wurtzite platelets may occur; however, a multiplicity of competing mechanisms appears to be operating, enabled by the higher growth temperature. These results will be reported separately. Figure 6 (a) shows the three types of matrix top surfaces typically present and Figures 6 (b)–(d) show examples of the nanowires and rods that grow from them. Nanowires are observed to grow from the fine and medium crystallite surfaces, but only rods are observed to grow from the large crystallite surfaces.

Figure 6 SEM investigations of the nanowire growth matrix at 1,000°C (a) three scales of growth matrix: types 1, 2 and 3 (b) nanowire (arrow) from fine crystallite matrix (c) nanowires (arrows) from medium crystallite matrix (d) a large tapered rod from large crystallite matrix (see online version for colours)

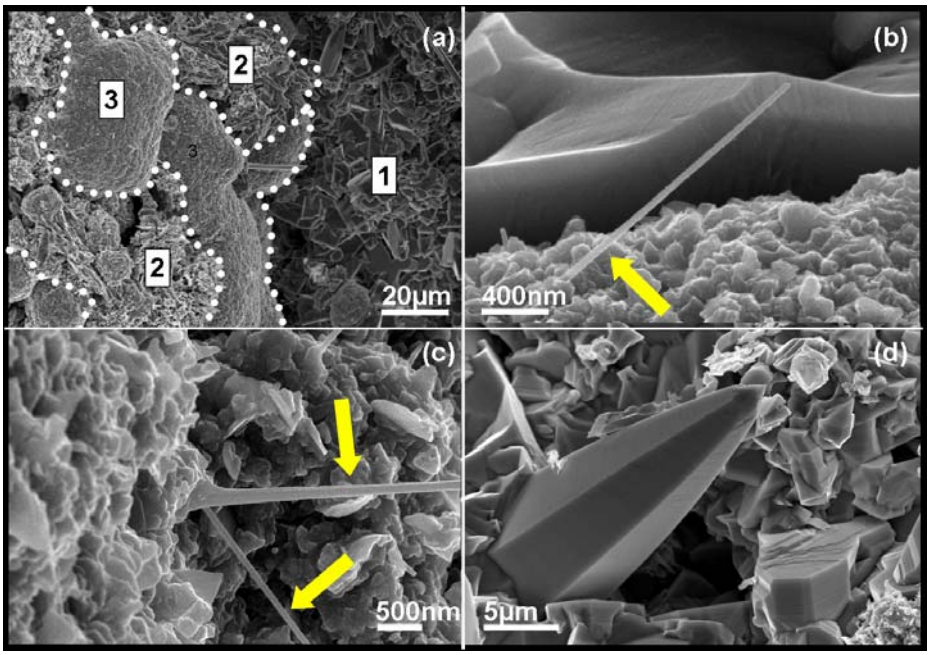

2.3 Electronic transport investigations

The effects of the internal structures on electronic transport were investigated by two-point microprobe and nanoprobe experiments. For these experiments, two terminal GaN nanocircuits were fabricated using electron beam lithography, using the multiphase nanowires grown at 850°C as active elements. GaN nanowires were first dispersed from an ethanol solution onto a silicon substrate with 100 nm of thermally grown silicon dioxide as an insulating layer. Source and drain contacts were patterned over the nanowires via EBL. Ti/Au (10/30 nm) was thermally evaporated for the conducting source and drain contacts after being exposed to a 100 W oxygen plasma (March Instruments PX-250) for 30 s to 1 min to remove any electron beam resist residue. Subsequent metal lift-off was performed in heated acetone. The EBL leads were connected to micron-scale contact pads previously fabricated using photolithography (PL) for the microprobe experiments.

The I–V characteristics of the GaN nanowire nanocircuits were first measured via the PL-fabricated contact pads (HP 4155C Semiconductor Parameter Analyser). V_{DS} was varied and the resulting current was measured. Figure 7(a) shows an SEM image of the nanowire contact region within a typical nanocircuit. The arrow shows the path of the induced current through the Ti/Au contacts and the nanowire.

Figure 7(b) shows a typical I–V curve. Over 70 µA was measured at 6 V_{DS}. The resulting curve was nonlinear with I proportional toV^2.

An additional nanocircuit was fabricated with three nanowires contacted in parallel. Over 400 μA was measured at 6 V_{DS}, as shown in Figure 8. This indicated that the current roughly scaled with the addition of two more nanowires. The resulting curve was nonlinear with I proportional to$V^{1.6}$.

Figure 7 (a) SEM of GaNFET nanocircuit (b) I–V characteristic

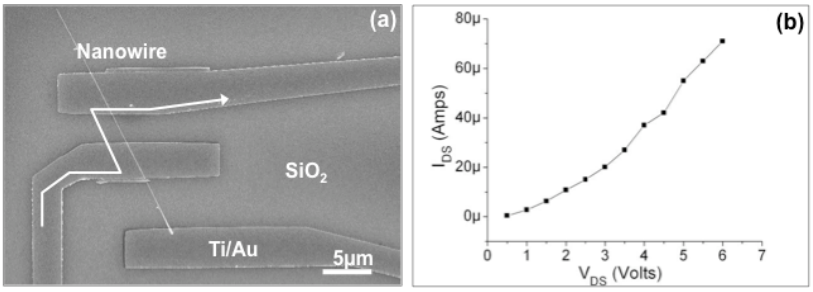

Note: Over 70 μA was measured at 6 V_{DS}.

Figure 8 GaN nanocircuit with three nanowires in parallel shows scaling of current to over 400 μA

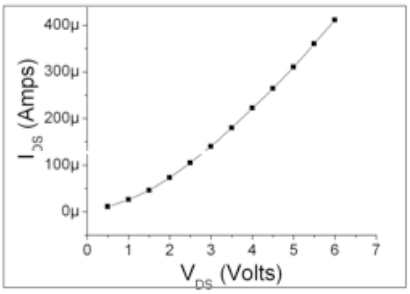

Further two-point probe investigations of the GaN nanowires in a two terminal device were carried out using a state-of-the-art nanoprobe instrument. The experiments were performed using a Zyvex KZ100 nanomanipulator system, which is a hybrid instrument interfacing the Keithley 4200-SCS and the Zyvex S100 nanomanipulator. It is equipped with NanoEffector® probes that are electrochemically etched tungsten polycrystalline wires with a nominal tip diameter of 50 nm, and is capable of probe positioning resolution within 5 nm. The small tip diameter and precise probe positioning allows direct nanoprobe-nanowire connections. The electronic characterisation with the KZ100 was performed in a LEO 1530 FESEM at room temperature, allowing real-time visual inspection with the SEM during the experiments. During measurements the SEM electron beam was turned off and during visual inspection with low acceleration voltage was used to minimise charge penetration effects. The tungsten probes were electrically cleaned in situ to provide a clean tungsten surface for the measurements.

In the two-point probe configuration the nanoprobes were first placed on the EBL fabricated metal contacts and the I–V characteristics were measured. The resulting curve was nonlinear with I proportional to$V^{1.7}$. The nanoprobes were then placed directly on the nanowire and the I–V characteristics were measured again. The resulting curve was also non-linear with I proportional to$V^{2.2}$.

Figure 9 I–V characteristic on GaN nanocircuit measured (a) with nanoprobes on the EBL fabricated metal contacts (b) with nanoprobes directly on the nanowire (see online version for colours)

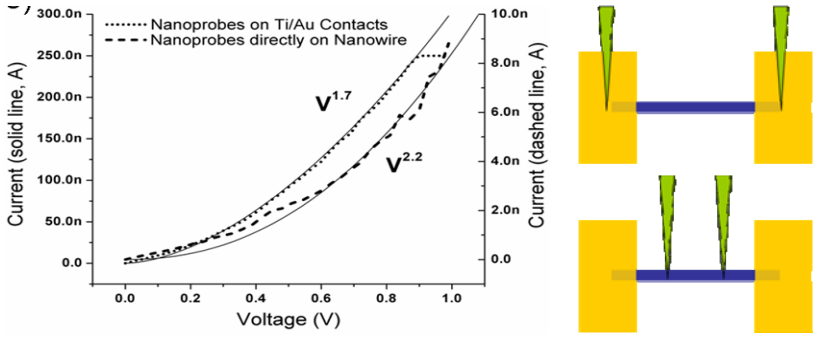

(a) (b)

The two-point microprobe and nanoprobe experiments all produced I–V characteristics which followed a power law dependence approximately given by I proportional toV^2. In every experiment, an exponential fit to the data was also investigated but proved to be an inferior fit. Non-linear I–V behaviour is typically observed in nanocircuits and is usually attributed to a Schottky barrier at the contacts. A double (two terminal) Schottky barrier would be expected to show an exponential dependence. However, a power law dependence can be attributed to space charge limited transport in the nanowire (Talin et al., 2008). The ~V^2 dependence can occur when there is low intrinsic doping, charge traps, or long depletion widths. Charge traps are related to surface states and the enhanced surface/bulk ratio in GaN nanowires in Talin et al. (2008). In the present investigations, the presence of additional internal surfaces has been demonstrated as well.

2.4 Contact resistance investigations

The electronic injection characteristics between metal electrodes and GaN nanowires in nanodevices are of great importance when maximising device performance, as these junctions play a critical role in device behaviour. Four-point nanoprobe investigations were carried out to quantify the contact resistances in a GaN nanowire device using the Zyvex KZ100 system. In the four-point probe measurements, the intrinsic nanowire resistance versus the Ti/Au-nanowire contact resistances were determined. This was done using floating voltage sense probes that were situated between two current source probes. This configuration is used to eliminate probe contact resistance effects so that the intrinsic nanowire resistance can be measured. The nanoscale voltage probes are important for four-point probe measurements of single-nanowire systems since they are less invasive than macroscopic probes and contacts. The 4200-SCS is also ideally suited for measurements in such nanoprobing configurations because it can make measurements with very low noise and can have input impedances greater than 10^{16} Ω.

Four separate four-point probe configurations were investigated to determine both total system and intrinsic nanowire resistance. In configuration A, the current source and voltage sense probes were placed on the Ti/Au contacts to measure the total system resistance. In configuration B, the current source probes were placed on the Ti/Au

contacts and voltage sense probes were directly contacted to the nanowire to investigate the nanowire resistance. In configuration C, the current source and voltage sense probes were directly contacted to the nanowire also to investigate the nanowire resistance. In configuration D, one current source probe was directly contacted at one end after breaking the nanowire, the voltage sense probes directly contacted the nanowire, and the other current source probe was placed on the Ti/Au contact. The open nanowire end contact was achieved through probe impact on the nanowire top surface, which resulted in a brittle fracture. This configuration was possible due to the probe tip diameter, which is around 50 nm, as it is comparable to the open nanowire cross-section width.

The four-point resistance measurements from configuration A, used to determine the total system resistance, consistently produced a resistance of between 3 and 6 MΩ, as shown in Figure 10(a), which is comparable to other reported findings. The graph also shows 'negative' data; this was a result of taking measurements in the opposite sense, i.e., a negative voltage, not a negative resistance. Measurements made in configurations B and C were used to determine the intrinsic nanowire resistance. In both configurations the nanowire resistance was between 500 and 800 kΩ, as shown in Figure 10(b). Probe coupling directly to the nanowire in these configurations appeared noisy at low source currents, but resistance values reduced to more consistent values at higher source currents. For a length of 16 μm between the voltage sense probes (directly observed in the SEM), and using a triangular base width and height of 100 nm, the resistivity was calculated to be 15.6 mΩ-cm. Configuration D was also used to determine nanowire resistance. After nanowire fracture to expose an end, the voltage sense probes were situated closer together at 10 μm, and the nanowire resistance was between 375 kΩ and 3 MΩ, as shown in Figure 10(c). It was noted that these data were the nosiest among all configurations; this was likely a result of the end-contacted configuration where stable coupling was more difficult to achieve.

Figure10 Four-point probe resistance measurements (a) Configuration A, total system resistance measurement, resistance values were between 3 and 5 MΩ (b) Configuration C, NW resistance measurement, side contact, resistance values were between 500 and 800 kΩ (c) Configuration D, NW resistance measurement, end contact, resistance values were between 375 kΩ and 3 MΩ (see online version for colours)

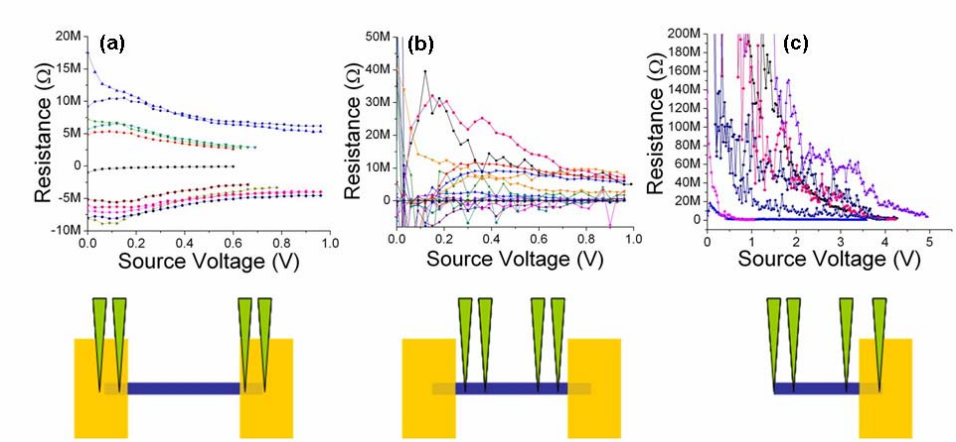

2.5 Implications for nanomanufacturing

To manufacture nanoscale devices with reproducible and reliable operation, a complete understanding of the nanomaterial characteristics and how all reduced dimensionality aspects operate within a device is essential. In this work, cross-section investigations revealed unexpected internal structures within highly crystalline nanowires that were not explicitly observable in plan-view HRTEM. Internal structures can impact optical and electronic properties, and should be investigated for different nanowire systems. Electronic transport investigations, using micro and nanoscale contact geometries, found a consistent power law dependence that indicated that space charge limited current may dominate transport in the multiphase GaN nanowire system. Carrier injection into nanowires has yet to be completely explained at a fundamental level, which impedes the effectiveness of device design. In this work, we have reported first contact resistance investigation, using nanoprobe contact geometries for the investigations, including direct nanoprobe-nanowire measurements. Work on the potential of nanoscale injection geometries is continuing in our group.

Acknowledgements

The support of NASA Goddard Space Flight Center, MEI Task No. 14 and the National Science Foundation IREE Program, grant DMI-0637134, are gratefully acknowledged. The authors thank Maoqi He and Joshua B. Halpern of Howard University for sourcing the nanowires used in this study. B.W. Jacobs thanks the NASA Graduate Student Researchers Program. FIB cross-sections were fabricated at the Electron Microbeam Analysis Laboratory (EMAL) at the University of Michigan.

References

Bierman, M.J., Lau, Y.K.A., Kvit, A.V., Schmitt, A.L. and Jin, S. (2008) *Science*, Vol. 320, pp.1060–1063.

Eshelby, J.D. (1953) *J. Appl. Phys.*, Vol. 24, pp.176–179.

Eshelby, J.D. and Stroh, A.N. (1951) *Phil. Mag.*, Vol. 42, pp.1401–1405.

Frank, F.C. (1951) *Acta Cryst.*, Vol. 4, pp.497–501.

Gradecak, S., Qian, F., Li, Y., Park, H-G. and Lieber, C.M. (2005) *Appl. Phys. Lett.*, Vol. 87, p.173111.

He, M., Zhou, P., Mohammad, S.N., Harris, G.L., Halpern, J.B., Jacobs, R., Sarney, W.L. and Salamanca-Riba, L. (2001) *J. Crys. Growth*, Vol. 231, pp.357–365.

Hersee, S.D., Sun, X. and Wang, X. (2006) *Nano Lett.*, Vol. 6, pp.1808–1811.

Huang, M.H., Mao, S., Feick, H., Yan, H., Wu, Y., Kind, H., Weber, E., Russo, R. and Yang, P. (2001) *Science*, Vol. 292, pp.1897–1899.

Jacobs, B.W., Ayres, V.M., Crimp, M.A. and McElroy, K. (2008a) *Nanotechnol.*, Vol. 19, p.405706.

Jacobs, B.W., Crimp, M. A.,McElroy, K., and Ayres, V. M. (2008b) *Nano Lett.*, Vol. 8, p.4354.

Jacobs, B.W., Ayres, V.M., Stallcup, R.E., A Hartman, A., Tupta, M.A., Baczewski, A.D., Crimp, M.A., Halpern, J.B., He, M., and Shaw, H.C. (2007a) *Nanotechnol.*, Vol. 18, p.475710.

Jacobs, B.W., Ayres, V.M., Petkov, M.P., Halpern, J.B., He, M., Baczewski, A.D., McElroy, K., Crimp, M.A., Zhang, J. and Shaw, H.C. (2007b) *Nano Lett.*, Vol. 7, pp.1435–1438.

Johnson, J.C., Choi, H-J., Knutsen, K.P., Schaller, R.D., Yang, P. and Saykally, R.J.(2002) *Nat. Mater.*, Vol. 1, pp.106–110.

Kuykendall, T., Pauzauskie, P.J., Zhang, Y., Goldberger, J., Sirbuly, D., Denlinger, J. and Yang, P. (2004) *Nat. Mater.*, Vol. 3, pp.524–528.

Mikkelsen, A., Sköld, N., Ouattara, L., Borgström, M., Andersen, J.N., Samuelson, L., Seifert, W. and Lundgren, E. (2004) *Nat. Mater.*, Vol. 3, pp.519–523.

Talin, A.A., Leonard, F., Swartzentruber, B.S., Wang, X. and Hersee, S.D. (2008) *Phys Rev Lett.*, Vol. 101, p.076802.

Tao, X. and Li, X. (2008) *Nano Lett.*, Vol. 8, pp.505–510.

Tham, D., Nam, C.Y. and Fischer, J.E. (2006) *Adv. Funct. Mater.*, Vol. 16, pp.1197–1202.